[SLAC-PUB-9347]
May 2002

Thermodynamic Interactions in Organometallic Block Copolymers *

Hany B. Eitouni, Nitash P. Balsara
Department of Chemical Engineering, and Material Sciences Division, Lawrence Berkeley National Laboratory, University of California, Berkeley, California 94720

Hyeok Hahn
Department of Chemical Engineering, University of California, Berkeley, California 94720

John A. Pople
Stanford Synchrotron Radiation Laboratory, Stanford Linear Accelerator Center, Stanford University, Stanford, CA 94309

Mark A. Hempenius
MESA$^+$ Research Institute and Faculty of Chemical Technology, University of Twente, P.O. Box 217, NL-7500 AE Enschede, The Netherlands

Abstract
The thermodynamic interactions in anionically synthesized poly(styrene-*block*-ferrocenyldimethylsilane) (SF) copolymers were examined using birefringence, small angle X-ray and neutron scattering (SAXS and SANS). We show that birefringence detection of the order-disorder transition is possible in colored samples provided the wavelength of the incident beam is in the tail of the absorption spectrum. The location of the order-disorder transition was confirmed by SAXS. The temperature-dependence of the Flory-Huggins parameter, χ, of SF copolymers, determined by SAXS, is similar in magnitude to that between polystyrene and polyisoprene chains. We find that χ is independent of block copolymer composition (within experimental error). We also demonstrate that the neutron scattering length densities of styrene and ferrocenyldimethylsilane moieties are identical due to a surprising cancellation of factors related to density and atomic composition.

Keywords
block copolymers; scattering; thermodynamic interactions; birefringence; SANS; SAXS; polymer structure

Submitted to Macromolecules

* Work supported by Department of Energy contract DE-AC03-76SF00515

Introduction

The spontaneous assembly of block copolymers into periodic structures with long-range order is a subject of considerable interest. Most of our quantitative understanding of block copolymer self-assembly is based on organic block copolymers and their response to changes in classical thermodynamic variables such as temperature, pressure, and solvent concentration. The factors that govern the formation of domains such as lamellae, cylinders arranged on a hexagonal lattice, and spheres arranged on a cubic lattice are well understood.[1-5] Recent interest in this field stems from the recognition that block copolymers may enable a wide variety of new applications ranging from high density information storage and photonic devices to nanofilters and catalysis.[6-8] These applications require organizing inorganic domains (e.g. information storage requires magnetic domains while photonic devices require domains with high refractive indices) within block copolymers. Such domains can be obtained by templating, i.e. replacing the organic domains by inorganic materials, or by synthesizing copolymers with inorganic blocks.[9-11] The success of such projects hinges on the development of a fundamental understanding of the interactions between organic and inorganic materials. While several elegant experiments demonstrating the potential applications of inorganic assemblies organized by block copolymers have been conducted,[11,12] quantitative characterization of the interactions between organic and inorganic blocks does not exist. In this paper we provide quantitative thermodynamic characterization of diblock copolymers with organometallic blocks.

A variety of tools have been used to study the thermodynamics of block copolymers. These include electron microscopy, small-angle X-ray (SAXS) and neutron

scattering (SANS), rheology, and optical birefringence. The introduction of inorganic domains may either diminish or enhance the applicability of these techniques. Inorganic materials exhibit absorption and low transmission at optical wavelengths, and thus techniques such as birefringence may not be effective for studying these materials. On the other hand, the high electron density of inorganic domains enables transmission electron microscopy of samples without staining (staining is almost always necessary for imaging domains of organic block copolymers).

Our work is based on the pioneering studies of Manners and coworkers who demonstrated methods for synthesizing block copolymers with an organometallic poly(ferrocenylsilane) block.[13-15] These materials are particularly interesting due to the redox activity of the ferrocene moieties as well as their interesting chemical and physical properties.[16] Poly(ferrocenylsilane)s, composed of alternating ferrocene and dialkylsilane units in the main chain, show electrostatic interactions between neighboring iron atoms in the charged state.[13,17,18] Intra- and inter-molecular interactions in these systems can thus be adjusted electrochemically or by the addition of charged species, thereby providing additional means to control order formation. The present work lays the foundation for studying such effects.

Lammertink et al. studied order formation in a series of poly(styrene-*block*-ferrocenyldimethylsilane) copolymers (SF) by transmission electron microscopy (without staining), SAXS, and rheology.[19] They identified phases that were similar to those found in conventional organic block copolymers. They also demonstrated that rheology could be used to locate order-disorder transitions in SF block copolymers.

In this paper we present data obtained by SAXS, SANS, and birefringence. In spite of the deep orange color of the diblock copolymer and low optical transmission coefficient, we show that the order-disorder transition can be probed by birefringence. The order-disorder transition temperature obtained by birefringence is in excellent agreement with that obtained from SAXS. The temperature-dependence of the SAXS data obtained from SF diblock copolymers above the order-disorder transition temperature was used to estimate the temperature dependence of the Flory-Huggins interaction parameter χ. We find χ to be independent of copolymer composition (within experimental error) and very similar in magnitude to that obtained in polystyrene-polyisoprene diblock copolymers. We thus demonstrate that frameworks previously developed for the study of interactions between organic polymer chains can be used to describe the interactions between organic and organometallic chains. We also demonstrate the neutron scattering length densities of polystyrene and poly(ferrocenyldimethylsilane) to be virtually identical. Thus, SANS cannot be used to study unlabeled SF copolymers.

Synthesis and Characterization of Polymers

Our method for synthesizing poly(styrene-*block*-ferrocenyldimethylsilane) copolymers is based on refs. 13, 14, 19 and 20. The chemical structure of the block copolymer is presented in Figure 1. Ferrocene (98%) was obtained from Acros. *n*-Butyllithium (1.6 M in hexanes), dibutylmagnesium (1.0 M in heptane), barium oxide, and calcium hydride were obtained from Aldrich and used as received. Ether and benzene were obtained from Aldrich and purified by distillation over sodium and *n*-

butyllithium, respectively. Burdick and Jackson brand tetrahydrofuran (THF) and heptane were obtained from VWR and purified by distillation over sodium and calcium hydride, respectively. N,N,N',N'-tetramethylethylenediamine (TMEDA, Aldrich, 99.5%) was distilled from barium oxide, and dichlorodimethylsilane (DMDCS, Aldrich, 99%) was distilled from calcium hydride prior to use. Styrene (Aldrich, 99%) was purified by distillation over dibutylmagnesium.

TMEDA was distilled into a solution of ferrocene in heptane, and *n*-butyllithium was syringed into the flask under argon. The mixture was allowed to react under argon for 48 hours. Due to air sensitivity, the supernatant was pipetted off in a glove box containing a prepurified argon atmosphere and the precipitate was washed with heptane. Ether was distilled into the flask with the dried precipitate. DMDCS was distilled into the chilled solution and allowed to stir for 12 hours. This led to the formation of our monomer 1,1'-dimethylsilylferrocenophane and lithium chloride. The solvent and other volatiles were distilled out of the reaction flask and the dried product was taken into the glove box. The 1,1'-dimethylsilylferrocenophane was dissolved in heptane and pipetted off of the lithium chloride precipitate. The 1,1'-dimethylsilylferrocenophane monomer was crystallized and sublimed twice to remove impurities prior to polymerization.

Three poly(styrene-*block*-ferrocenyldimethylsilane) copolymers were synthesized under high vacuum in benzene, using *n*-butyllithium as the initiator and methanol as the terminator. For each copolymer the polystyrene (S) block was synthesized first followed by the poly(ferrocenyldimethylsilane) (F) block by anionic and anionic ring opening polymerization, respectively. An aliquot of the reaction mixture containing the living polystyrene precursor chains was isolated and terminated to obtain the molecular weight

of the first block. The molecular weight of the polystyrene block was determined by GPC measurements using a Waters 2690 Seperations Module and a Viscotek Triple Detector system calibrated with polystyrene standards. The composition of the diblocks was obtained by ^{1}H NMR spectroscopy. The polymers studied are designated SF(9-14), SF(13-8), and SF(18-8) where the numbers in parenthesis refer to the number averaged molecular weights in kg/mol of the S and F blocks, respectively. The polydispersities of the copolymers were obtained from GPC measurements using a polystyrene calibration curve. The GPC chromatogram of SF(9-14) indicated the presence of the copolymer as well as unreacted homopolystyrene, formed presumably by termination of some of the polystyrene precursor chains by impurities in the F monomer. The homopolystyrene was easily eliminated by fractionation, using toluene and methanol as the solvent and non-solvent, respectively. We also synthesized a polystyrene-*bloc*k-polyisoprene copolymer [SI(8-24)] using procedures described in ref. 21. This sample served as a reference because the thermodynamic properties of SI copolymers are well known. Samples were freeze-dried from benzene solutions to ensure complete dryness of the polymers before experimental use.

DSC scans on a TA 2920 instrument at 10 °C/min for the SF polymers in the range of 0 to 170 °C revealed two glass transitions. The first glass transition, corresponding to the F block, was observed at approximately 30 °C while the second glass transition, corresponding to the S block, occurred at approximately 80 °C. Because no crystalline melting peaks were observed, the density of the F block was assumed to be that of the amorphous polymer, 1.26 g/cm^3.[19] UV-visible spectroscopy of the SF samples was performed using a Cary 400Bio UV-Visible spectrometer. A typical UV-vis

spectrum [SF(13-8)], shown in Figure 2, shows that light in the range of wavelengths from 600 to 800 nm is transmitted, as expected by the red-orange color of the polymers. The absorbance peak at 258 nm corresponds to the aromatic ring of polystyrene and the peak at 455 nm corresponds to the disubstituted ferrocene (Figure 2). The characteristics of the polymers used in this study are summarized in Table 1.

The optical birefringence of the samples was determined using an instrument described previously.[22] The samples were illuminated with a plane polarized light beam of wavelength 633 nm. The fraction of the incident power reaching the detector after passing through the sample held between crossed polarizers, P/P_0, was recorded (P is the transmitted power and P_0 is the incident power).

Small angle X-ray scattering (SAXS) was also performed on the SF(13-8), SF(9-14), SF(18-8), and SI(8-24) melts over a range of 50 to 220 ºC. Two-dimensional SAXS patterns from the SF copolymers were obtained from ca. 0.2 mm thick samples. The thickness of the SI(8-24) sample was 1 mm. SAXS experiments were performed on beamline 1-4 of the Stanford Synchrotron Radiation Laboratory (SSRL). The beamline was configured with X-rays of wavelength 1.488 Å ($\Delta\lambda/\lambda \sim 1\%$) focused independently in the horizontal and vertical planes to give a beam size of ~0.5 mm diameter. The polymers were held in aluminum sample cells, which sealed them from contact with the air, and the probe beam was transmitted through Kapton windows in the cell. Two-dimensional X-ray scattering patterns were collected on a CCD based X-ray detector with a 100 mm diameter. The two dimensional scattering patterns were radially averaged, corrected for dark current in the CCD and scattering from air and the windows in the cell, and converted to absolute intensities using standards provided by SSRL. We report the

absolute SAXS intensity I as a function of scattering vector q ($q=4\pi\sin(\theta/2)/\lambda$ where θ is the scattering angle and λ is the wavelength of the incident X-rays).

Small-angle neutron scattering (SANS) measurements were conducted on 1 mm thick samples encased between quartz windows on the 30 m beam line (NG3) at the National Institute of Standards and Technology in Gaithersburg, MD. Two-dimensional SANS patterns were measured as a function of scattering angles with the following instrument configuration: neutron wavelength, λ = 6 Å, wavelength spread, $\Delta\lambda/\lambda$ = 0.15, sample-to-detector distance = 5 m, sample aperture = 1.27 cm, source to sample distance = 14.7 m, and source size = 5 cm. We report the radially averaged measured SANS intensity I_{SANS} (in arbitrary units) versus scattering vector q (definition of q is identical to that used for SAXS).

Birefringence Detection of the Order-Disorder Transition

The use of birefringence as a means of studying the order to disorder transition (ODT) has been well established both experimentally and theoretically.[22-26] It has been shown that a sample consisting of randomly oriented grains of ordered lamellae or cylinders, when illuminated with plane-polarized light, will transmit a fraction of the incident power through a crossed polarizer.[22,25] Previous studies were conducted on transparent samples, i.e. transmission coefficient equal to unity. The signal from a sample with a transmission coefficient that is less than unity will be affected by absorption and possible linear dichroism due to alignment of the absorbing moieties. For the simple case where linear dichroism effects are negligible, the fraction P/P_0 is given by

$$\frac{P}{P_0} = \frac{4\pi^2}{15}(\Delta n)^2 \frac{L l_{av}}{\lambda^2} e^{-cL} \qquad (1)$$

where Δn is the difference in refractive indices for light polarized parallel and perpendicular to the optic axis of a single grain, L is the sample thickness, l_{av} is the characteristic size of the grains, λ is the wavelength of light used, and c is the absorption coefficient. Equation 1 is valid for weakly birefringent systems with P/P_0 much less than unity. Since P/P_0 must be nearly zero in the disordered state (both Δn and l_{av} are zero in eq 1), the ODT can be identified by a discontinuous drop of P/P_0 to zero, provided the attenuation of the signal due to absorbance is not severe.

The dried polymers were sealed in quartz cuvettes with path lengths of either 0.2 mm or 1 mm and annealed to remove any bubbles. A simple transmission measurement revealed that c=0.92 mm^{-1} for SF(9-14) and 1.05 mm^{-1} for SF(13-8). This is considerably different from organic block copolymers wherein c≈0.[21,25] Note 633 nm (the wavelength of the incident laser) is in the tail of the poly(styrene-*block*-ferrocenyldimethylsilane) absorption peak (Figure 2). While there is considerable absorption at λ=633 nm, it does not rule out the possibility of studying order-disorder transitions in SF block copolymers. The samples were subjected to a series of temperature jumps starting near room temperature. The steady state P/P_0 obtained at different temperatures are shown in Figure 3. The time required to reach a steady state signal after each jump was about 30 minutes. For SF(9-14) the value of P/P_0 at temperatures in the vicinity of 100 °C is $5x10^{-3}$. This is an order of magnitude smaller than typical signals obtained from SI copolymers.[27] A factor of 3 decrease is expected due to absorption alone. The remaining differences may

be due to differences in grain structure (Δn and l_{av} terms in eq 1). Between 156 and 161 ºC there is an abrupt decrease in P/P_0 by about an order of magnitude (from $1x10^{-2}$ to $7x10^{-4}$). The thermal history imposed upon the sample affects the grain structure and thus P/P_0. Several thermal histories were imposed upon the SF(9-14) and in each case the P/P_0 signal converged to zero between 156 and 161 ºC indicating that the ordered structure was destroyed at the same temperature regardless of thermal history. We thus conclude that the order-disorder transition temperature (T_{ODT}) of SF(9-14) is 159 $\pm$ 3 ºC. Also shown in Figure 3 is the temperature dependence of P/P_0 of SF(13-8), which is relatively constant with temperature and nearly zero [$(5\pm2)x10^{-4}$]. We conclude that SF(13-8) is disordered across the accessible temperature range.

Small Angle X-ray and Neutron Scattering

In Figure 4 we show the SAXS profiles I(q) at selected temperatures from SF(9-14). At room temperature the first and second order peaks corresponding to a lamellar structure are evident in I(q); see inset in Figure 4. A qualitative change in the scattering profiles is seen between 157 and 167 ºC indicating an order-to-disorder transition (T_{ODT} = 162 $\pm$ 5 ºC). In Figure 5 we show the SAXS profiles I(q) at selected temperatures from SF(13-8). We see no abrupt changes in peak width in our temperature window indicating the absence of an order-disorder transition. These results are consistent with the results of the birefringence experiments (Figure 3).

In Figure 6 we show the temperature dependence of the peak width at half height for both SF(9-14) and SF(13-8). We focus on samples in the molten state (above T_g) where equilibration is expected. The peak width of SF(9-14) increases abruptly from

0.06 to 0.1 nm^{-1} between 157 and 167 ºC [at T_{ODT}]. In contrast the peak width of SF(13-8) is broad at all accessible temperatures and is similar to that obtained from SF(9-14) in the disordered state. The SAXS data reinforce earlier conclusions regarding the state of SF(13-8) and SF(9-14).

In Figure 7 we show the temperature dependence of the main characteristics of the scattering profiles, the peak intensity I_{MAX}. The data in the ordered state are represented by open symbols, while the data in the disordered state are represented by filled symbols. The peak intensities of the two SF copolymers in the disordered state are comparable. The scattering intensity from SI(8-24) in both ordered and disordered states is substantially lower than that of the corresponding states of the SF copolymers [note that the SI(8-24) data in Figure 7 show a step change at the ODT]. This may be due to the enhanced scattering contrast between the F and S blocks and/or enhanced microphase separation due to the incompatibility between the F and S blocks. We resolve these effects by a detailed analysis of the SAXS profiles in the disordered state.

The q-dependence of the scattering intensity (measured either by SANS or SAXS) from a disordered block copolymer melt, within the random phase approximation (RPA), obtained by Leibler,[1] is given by:

$$I(q) = \left(\frac{b_1}{v_1} - \frac{b_2}{v_2} \right)^2 \left\{ \frac{S_{11}^o + S_{22}^o + 2S_{12}^o}{S_{11}^o \cdot S_{22}^o - (S_{12}^o)^2} - \frac{2\chi}{v} \right\}^{-1} \qquad (2)$$

where the subscripts 1 and 2 refer to the two blocks, b_i and v_i are the scattering lengths and volumes, χ is the Flory-Huggins interaction parameter based on reference volume v,

which we set to 100 Å^3, and S_{ij}^o are the ideal correlations between blocks i and j in the absence of interactions.

$$S_{ii}^o = \phi_i N_i v_i P_i(q) \qquad (i = 1,2) \tag{3a}$$

$$S_{12}^o = (\phi_1 N_1 v_1 \phi_2 N_2 v_2)^{1/2} \cdot F_1(q) \cdot F_2(q) \tag{3b}$$

N_i is the number of monomers in block i, ϕ_i is the volume fraction of the block, and v_i is the volume of monomer i.[28] $P_i(q)$ and $F_i(q)$ are the intrablock and interblock correlations, described by the Debye and the Leibler functions, respectively:

$$P_i(q) = 2\frac{\exp(-u_i) - 1 + u_i}{u_i^2} \qquad (i = 1,2) \tag{4a}$$

$$F_i(q) = \frac{1 - \exp(-u_i)}{u_i} \qquad (i = 1,2) \tag{4b}$$

where $u_i = q^2 N_i l_i^2/6$ and l_i is the statistical segment length of block i.

The main features of the scattering profiles from disordered SF(9-14) and SF(13-8) were fit to eq 2 using χ and l_i as adjustable parameters. Following procedures established in ref. 21, the heights of the experimental and theoretical peaks (I_{MAX}) were matched by adjusting χ while the location of the peak in q-space was obtained by adjusting an averaged statistical segment length $l = l_1 = l_2$. All other parameters in eq 2 were obtained from polymer characterization experiments and can be found in Tables 1 and 2. In Figure 8 we compare typical I(q) data obtained from disordered SF(9-14) with

eq 2 with χ and l as adjustable parameters.[1] The experimental peaks are considerably broader than the theoretical predictions due to instrumental smearing. The protocols for correcting for this effect have not yet been determined for the SAXS instrument. However, in our previous studies on block copolymer thermodynamics using SANS,[21] we had studied the effect of instrumental smearing and found that the χ and l parameters obtained from measured and corrected data were less than 1%. We were able to gauge the importance of smearing corrections by analyzing the data obtained from SI(8-24). Fitting SAXS data from SI(8-24) in the disordered state, we obtain the temperature dependence of χ between polystyrene and polyisoprene (triangles shown in Figure 9). A least squares linear fit of the data gives

$$\chi = 0.027 + 3.61/T \qquad \text{for SI(8-24)} \tag{5}$$

where T is expressed in Kelvin. Our expression for χ of SI(8-24) (eq 5) is within 10% of χ parameters for SI copolymers determined by SANS experiments wherein effects of instrumental smearing were taken into account.[21] We thus conclude that our estimate of χ from SAXS is not seriously affected by instrumental smearing.

The χ parameters required to fit the SAXS data from disordered SF(9-14) and SF(13-8) are also shown in Figure 9. It is evident that the χ parameters are approximately linear functions of 1/T. The following equations represent linear least squares fits through SF copolymer data sets.

$$\chi = 0.023 + 3.68/T \qquad \text{for SF(9-14)} \tag{6a}$$

$$\chi = 0.028 + 3.28/T \quad \text{for SF(13-8)} \tag{6b}$$

Also included in Figure 9 are the only estimates of χ between S and F chains that we were able to extract from the literature. The data are based on the work of Li et al.[29] who found that the sphere-to-disorder transition temperature of an SF diblock copolymer was 220 ºC and on the work of Lammertink et al.[19] who found that the cylinder-to-disorder transition temperature of an SF diblock copolymer was 175 ^{o}C. In our nomenclature, their polymers would be called SF(9-27) and SF(17-8), respectively. For SF(9-27) the value of ϕ_s was 0.31 and N, the number of monomers per chain, was 494 based on a 100 Å^3 reference volume; while for SF(17-8), ϕ_s was 0.71 and N was 411. Li et al. reported that χN=17.5 at the transition temperature based on the fluctuation-corrected theory of Fredrickson and Helfand,[30] which indicates that χ=0.035 at 220 ºC. Considering the work of Lammertink et al., the formation of cylinders in Leibler's theory[1] occurs at χN=15.4 (we ignore the spherical phase predicted incorrectly by the Leibler theory), which indicates that χ=0.037 at 175 ^{o}C. Using the same framework, the value of χ at the ODT of SF(9-14), calculated to be 0.0310, agrees remarkably well with eq 6a which gives 0.0315 at T_{ODT} = 162 ºC. For SF(13-8) the calculated temperature for order formation estimated using eq 6b is below 0 Kelvin, indicating that SF(13-8) is well-removed from an order-disorder transition.

It is clear from Figure 9 that χ parameters of our SF(9-14) and SF(13-8) copolymers and that of SF(17-8) taken from ref. 19 and SF(9-27) taken from ref. 29 are within experimental error. It is therefore evident that concepts such as χ parameters, used routinely as a gauge of interaction strength between organic polymer chains, are also

applicable to interactions between organic and organometallic chains. Further, the repulsive interactions between polystyrene and poly(ferrocenyldimethylsilane) (S and F) chains are nearly identical in magnitude to those between polystyrene and polyisoprene. We had expected significantly larger repulsion between S and F due to the presence of Fe and Si atoms on the poly(ferrocenyldimethylsilane) chains. Perhaps, the relatively weak repulsion that we see between S and F chains is due to the fact that both the Si and Fe atoms in the F chains are surrounded by hydrocarbon moieties (see Figure 1). It is thus clear that the large differences in I_{MAX} of SI and SF chains noted in Figure 7 arises entirely due to changes in scattering contrast and not due to differences in thermodynamic interactions.

In Figure 10 we show the temperature dependence of l for SF(9-14), SF(13-8), and SI(8-24). The average statistical segment length of the SF copolymers is significantly larger than that of SI copolymers, presumably due to the stiffness of the F block. We thus attribute the large l of SF(9-14) relative to SF(13-8) to the fact that the volume fraction of the F monomers in SF(9-14) is larger. If we assume that the statistical segment length of the PS chains in both SI and SF copolymers is 0.57 nm (at 167 °C for a 100 $Å^3$ monomer)[27] and adjust the statistical segment length of the F block to match the peak location in the SAXS data, then the statistical segment length of the F chains is estimated to be 1.53 nm in SF(9-14), and 2.12 nm in SF(13-8). In all three systems, the weak temperature dependence of l, seen in Figure 10, can be approximated by a straight line. The temperature coefficient of l (dl/dT) for SF(13-8) is –0.0011 nm/K, while that for SF(9-14) is 0.005 nm/K. The value obtained for SI(8-24), -0.0013 nm/K, is in reasonable agreement with values obtained from similar polymers by SANS.[21]

In Table 2 we show the calculated scattering length densities (b_i/v_i) of polystyrene, poly(ferrocenyldimethylsilane) and polyisoprene for neutron scattering. The scattering length density difference between hydrocarbon chains such as polystyrene and polyisoprene is partly due to differences in density. The density difference between polystyrene and poly(ferrocenyldimethylsilane) is significantly larger than that between polystyrene and polyisoprene. In addition, the scattering lengths of Si and Fe are quite different from C and H. These differences are exploited routinely in SANS experiments, e.g. studies of silica suspensions in hydrocarbon solvents.[31] One might thus expect a substantial neutron contrast between the polystyrene and poly(ferrocenyldimethylsilane) blocks in SF polymers. This is, however, not the case. The neutron scattering length density difference between polystyrene and poly(ferrocenyldimethylsilane) is about 2 orders of magnitude lower than that between polystyrene and polyisoprene (with neither chain labeled with deuterium). This is due to an unexpected compensation of effects due to differences in density and atomic composition of the monomers. We confirmed this experimentally by conducting a quick SANS run on SF(18-8). The SANS profile from this sample showed no evidence of structure, as can be seen from the q-independent data shown in Figure 11a.[32] Based on the χ parameter between F and S blocks we expect SF(8-18) to be deep in the ordered regime. The SAXS intensity profile of SF(8-18), presented in Figure 11b, confirms this. The large SAXS intensity and the presence of primary and higher order peaks clearly indicate the existence of a cylindrical phase. This unexpected SANS contrast match could be exploited in studies of multicomponent blends containing polystyrene and poly(ferrocenyldimethylsilane) chains.

Concluding Remarks

We have studied the thermodynamic interactions between hydrocarbon and organometallic chains in poly(styrene-*block*-ferrocenyldimethylsilane) copolymers using birefringence, SAXS and SANS. We find that birefringence detection of the order-disorder transition in these samples is not precluded by visible absorption provided the wavelength of the incident beam is in the tail of the absorption spectrum. To our knowledge, the applicability of the birefringence technique[25] to colored samples has not been demonstrated previously. The location of the order-disorder transition was also determined by SAXS and found to be consistent with the birefringence results. The χ parameter between polystyrene and poly(ferrocenyldimethylsilane) chains, determined by fitting the scattering function obtained by Leibler to the SAXS data of the disordered samples, is similar to that between polystyrene and polyisoprene chains and is independent of block copolymer composition. We show that the neutron scattering length densities of polystyrene and poly(ferrocenyldimethylsilane) are matched due to an unexpected cancellation of factors related to density and atomic composition.

Acknowledgment

This work is supported by the U.S. Department of Energy (Basic Energy Sciences), and conducted within the Polymer Program of the Materials Sciences Division at Lawrence Berkeley National Laboratory. We acknowledge the support of the National Institute of Standards and Technology, U.S. Department of Commerce, in providing facilities used in this work. This material is based upon

activities supported by the National Science Foundation under Agreement No. DMR-9986442.

References

(1) Liebler, L. *Macromolecules* **1980**, 13, 1602.

(2) Bates, F. S.; Rosedale, J. H.; Fredrickson, G. H. *J. Chem. Phys*. **1990**, 92, 6255.

(3) Sakamoto, N.; Hashimoto, T. *Macromolecules* **1995**, 28, 6825.

(4) Khandpur, A. K.; Forster, S.; Bates, F. S.; Hamley, I. W.; Ryan, A. J.; Bras, W.; Almdal, K.; Mortensen, K. *Macromolecules* **1995**, 28, 8796.

(5) Hamley, I. W. *The Physics of Block Copolymers*; Oxford University Press: New York, NY, 1998.

(6) Park, M.; Harrison, C.; Chaikin, P. M.; Register, P. A.; Adamson, D. H. *Science* **1997**, 276, 1401.

(7) Thurn-Albrecht, T.; Schotter, J,; Kastle, G. A.; Emley, N.; Shibauchi, T.; Krusin-Elbaum, L.; Guarini, K.; Black, C. T.; Touminen, M. T.; Russell, T. P. *Science* **2000**, 290, 2126.

(8) Segalman, R. A.; Yokoyama, H.; Kramer, E. J. *Adv. Mater*. **2001**, 13, 1152.

(9) Lammertink, R.G.H.; Hempenius, M.A.; Chan, V.Z.-H.; Thomas, E.L.; Vancso, G.J. *Chem. Mater.* **2001**, *13*, 429.

(10) Lammertink, R.G.H.; Hempenius, M.A.; Van den Enk, J.E.; Chan, V.Z.-H.; Thomas, E.L.; Vancso, G.J. *Adv. Mater.* **2000**, *12*, 98.

(11) Cheng, J.Y.; Ross, C.A.; Chan, V.Z.-H.; Thomas, E.L.; Lammertink, R.G.H.; Vancso, G.J. *Adv. Mater.* **2001**, *13*, 1174.

(12) Sohn, B. H.; Cohen, R. E. *Acta Polymer* **1996**, 47, 340.

(13) Rulkens, R.; Lough, A.J.; Manners, I. *J. Am. Chem. Soc.* **1994**, *116*, 797.

(14) Ni,Y.; Rulkens, R.; Manners, I. *J. Am. Chem. Soc.* **1996**, *118*, 4102.

(15) Kulbaba, K.; Manners, I. *Macromol. Rapid Commun.* **2001**, *22*, 711.

(16) Gallardo, B. S.; Gupta, F. D.; Jong, L. I.; Craig, V. S.; Shah, R. R.; Abbott, N. L. *Science* **1999**, 283, 57.

(17) Foucher, D. A.; Honeyman, C. H.; Nelson, J. M.; Tang, B. Z.; Manners, I. *Angew. Chem. Int. Ed. Engl.* **1993**, *32*, 1709.

(18) Nguyen, M. T.; Diaz, A. F.; Dement'ev, V. V.; Pannell, K. H. *Chem. Mater.* **1993**, *5*, 1389.

(19) Lammertink, R. G. H.; Hempenius, M. A.; Thomas, E. L.; Vancso, G. J. *J. Polym. Sci., Polym. Phys. Ed.* **1999**, 37, 1009.

(20) Fischer, A. B.; Kinney, J. B.; Staley, R. H.; Wrighton, M. S. *J. Am. Chem. Soc.* **1979**, 101, 6501.

(21) Lin, C. C.; Jonnalagada, S. V.; Kesani, P. K.; Dai, H. J.; Balsara, N. P. *Macromolecules* **1994**, 27, 7769.

(22) Garetz, B. A.; Newstein, M. C.; Dai, H. J.; Jonnalagadda, S. V.; Balsara, N. P. *Macromolecules* **1993**, 26, 3151.

(23) Amundson, K. R.; Helfand, E.; Patel, S. S.; Quan, X.; Smith, S. S. *Macromolecules* **1992**, 25, 1935.

(24) Balsara, N. P.; Perahia, D.; Safinya, C. R.; Tirrell, M.; Lodge, T. P. *Macromolecules* **1992**, 25, 3896.

(25) Balsara, N. P.; Garetz, B. A.; Dai, H. J. *Macromolecules* **1992**, 25, 6072.

(26) Milner, S. T. *Macromolecules* **1993**, 26, 2974.

(27) Balsara, N. P.; Lin, C. C.; Dai, H. J.; Krishnamoorti, R. *Macromolecules* **1994**, 27, 1216.

(28) The temperature dependence of the monomer volumes are available in the literature except for the case of poly(ferrocenyldimethylsilane). Lacking a better alternative, we used the thermal expansion coefficient of polystyrene to calculate monomer volumes for both blocks.

(29) Li, W.; Sheller, N.; Foster, M. D.; Balaishis, D.; Manners, I.; Annis, B; Lin, J. -S. *Polymer* **2000**, 41, 719.

(30) Fredrickson, G. H.; Helfand, E. *J. Chem. Phys.* **1987**, 87, 697.

(31) Newstein, M.C.; Wang, H.; Balsara, N.P.; Lefebvre, A.; Watanabe, H.; Osaki, K.; Shikata, T.; Niwa, H.; Morishima, Y., J. Chem. Phys, 1999, 111, 4827.

(32) Due to limitations of the temperature controlling device at the SAXS instrument, data below 50 °C could not be readily obtained. In Figure 11b we show data from SF(18-8) obtained at this temperature. We conducted SANS experiments on SF(18-8) at temperatures 25 °C and 150 °C, and saw data that was qualitatively similar to that shown in Figure 11a. The data in Figure 11a was obtained at 25 °C.

Table 1. Characteristics of Polymers Used in this Study

Sample Designation	Mn of S block (g/mol)	Mn of F (or I) block (g/mol)	Mw/Mn	ϕ_S	Tg 1 onset ºC	Tg 1 endpoint ºC	Tg 2 onset ºC	Tg 2 endpoint ºC
SF(9-14)	9000	13800	1.03	0.46	24	31	62	75
SF(13-8)	12500	8400	1.10	0.66	28	36	84	95
SF(18-8)	17900	7600	1.10	0.76	25	34	84	94
SI(8-24)	7500	24000	1.02	0.22	37	59	-	-

Table 2. Scattering Length Density of Chains for Neutrons and X-rays at 25 ºC

polymer	neutron, b/v (m^{-2})	X-ray, b/v (m^{-2})	v ($Å^3$)
polystyrene	1.384×10^{14}	9.500×10^{14}	168
poly(ferrocenyldimethylsilane)	1.285×10^{14}	1.126×10^{15}	319
polyisoprene	2.742×10^{14}	2.214×10^{15}	121

Figure Captions

Figure 1. Schematic representation of the chemical structure of SF diblock copolymers.

Figure 2. UV-visual absorbance spectrum of SF(13-8).

Figure 3. Birefringence detection of the order-disorder transition of SF(9-14) and SF(13-8): P/P_0, the fraction of transmitted light through a 1 mm thick sample held between crossed polarizers, versus temperature.

Figure 4. SAXS intensity profiles of SF(9-14). The order-disorder transition temperature is between 157 and 167 ºC. The inset obtained at 21 ºC shows higher order peaks corresponding to the lamellar phase.

Figure 5. SAXS intensity profiles of SF(13-8). The sample is disordered at all temperatures observed.

Figure 6. Peak width of SAXS intensity profiles of SF(9-14) and SF(13-8). The abrupt decrease in the peak width of SI(9-14) occurs at the order-disorder transition.

Figure 7. Peak intensity I_{MAX} versus temperature of SF and SI copolymers. SF(9-14): squares, SF(13-8) circles, SI(8-24): triangles. The filled symbols correspond to the data

taken in the disordered state while the unfilled symbols correspond to data taken in the ordered state. The RPA fits in this paper were conducted on the disordered state data.

Figure 8. RPA (eq 2) fit of SAXS data for SF(9-14) taken at 167 ºC with χ and l as the adjustable parameters.

Figure 9. Flory-Huggins interaction parameters χ based on the RPA fits of the SAXS data. Data from Lammertink et al.[19] and Li et al.[29] have been included. The reference volume is 100 $Å^3$. Error bar represents average uncertainty.

Figure 10. The average statistical segment lengths used to match the position of the SAXS peak in the disordered state to RPA-based calculations.

Figure 11. A comparison of (a) SANS and (b) SAXS profiles of SF(18-8).[32] The q-independent SANS data is due to a contrast match.

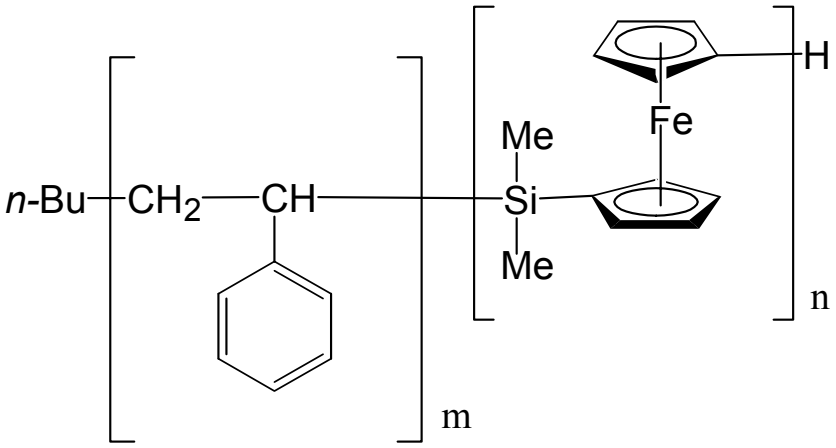

Figure 1

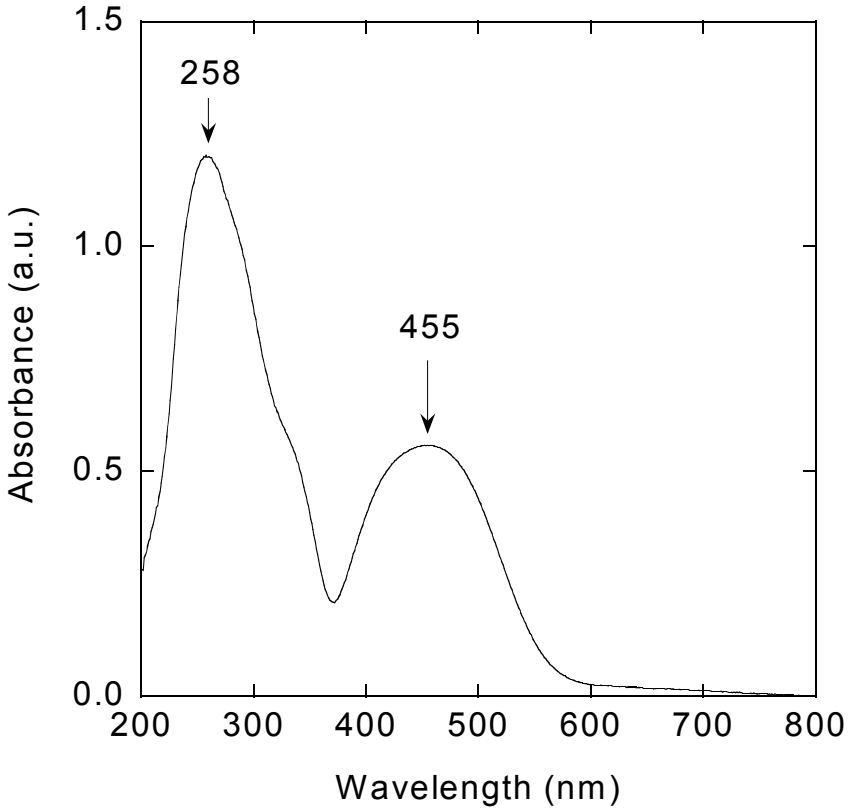
1.5
1.0
0.5
0.0
Absorbance (a.u.)
258
455
200
300
400
500
600
700
800
Wavelength (nm)

Figure 2

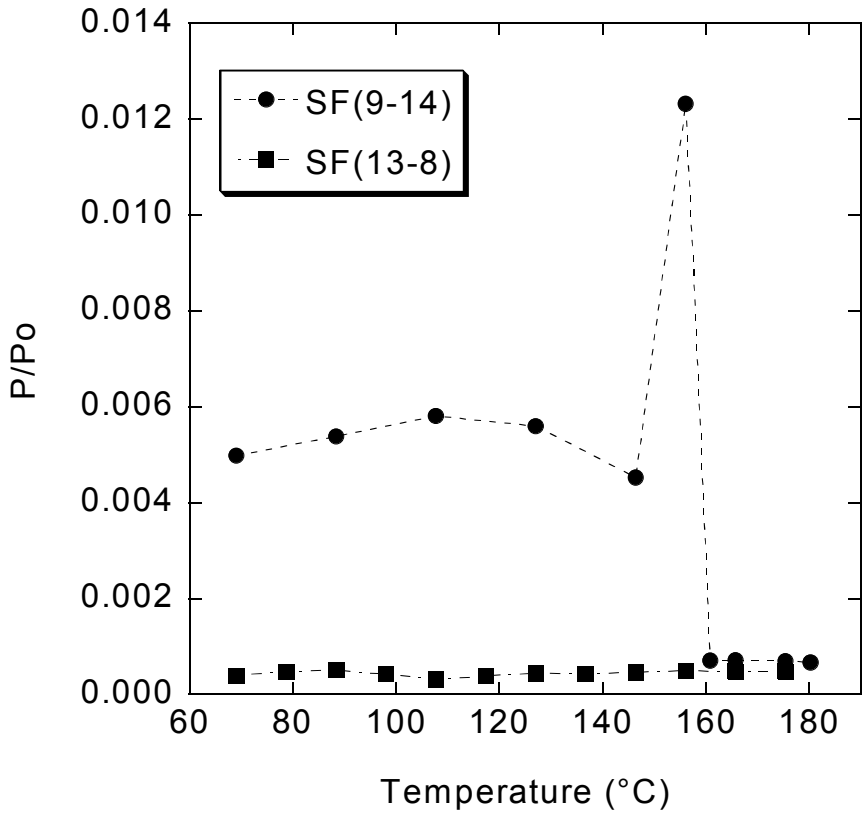
0.014
0.012
0.010
0.008
0.006
0.004
0.002
0.000
P/Po
SF(9-14)
SF(13-8)
60
80
100
120
140
160
180
Temperature (°C)

Figure 3

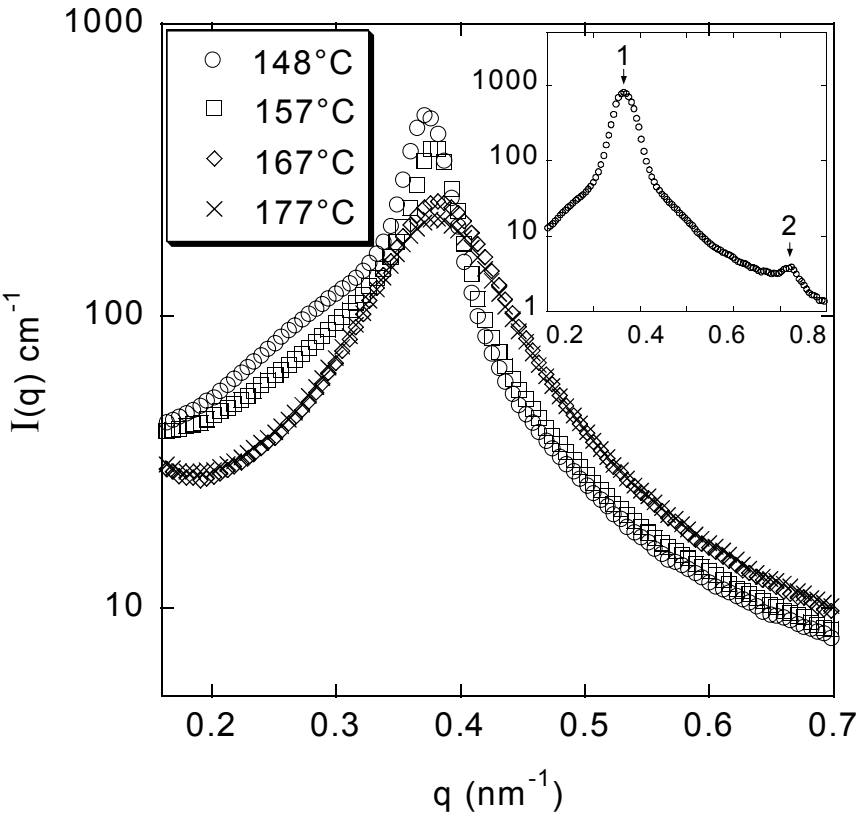
148°C
157°C
167°C
177°C
1000
100
10
I(q) cm-1
0.2
0.3
0.4
0.5
0.6
0.7
q (nm-1)
1
2
1000
100
10
1
0.2
0.4
0.6
0.8

Figure 4

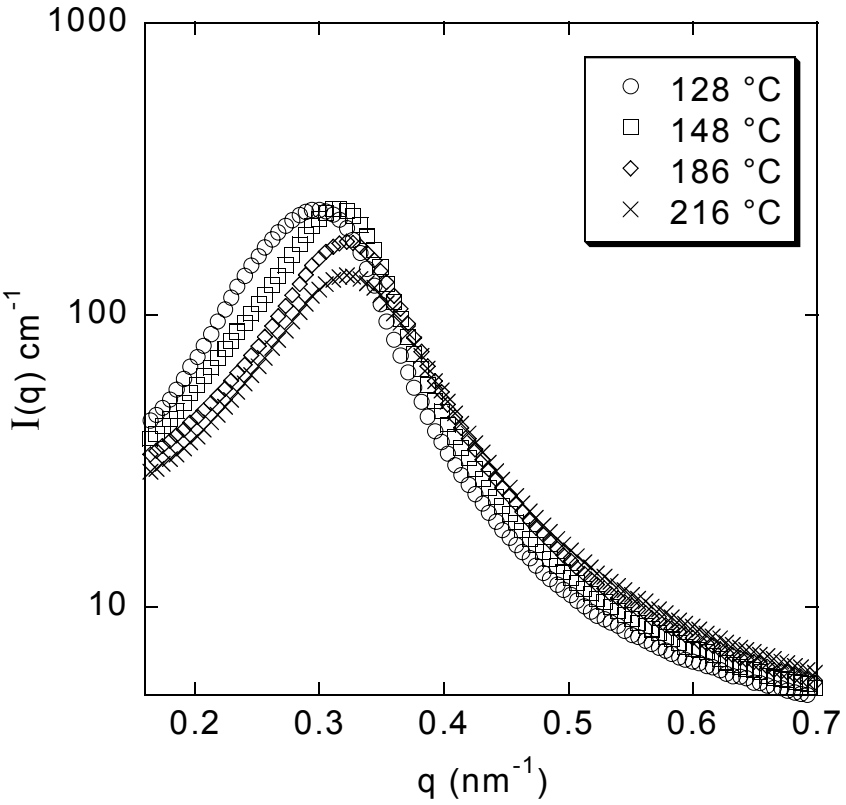

Figure 5

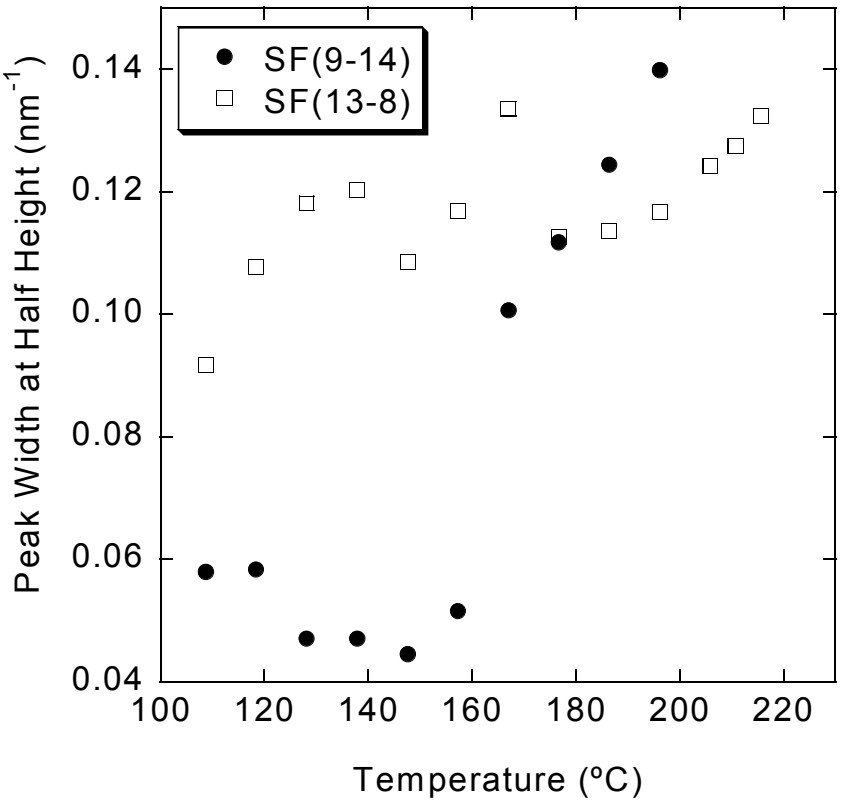
SF(9-14)
SF(13-8)
Peak Width at Half Height (nm^{-1})
0.14
0.12
0.10
0.08
0.06
0.04
100
120
140
160
180
200
220
Temperature (ºC)

Figure 6

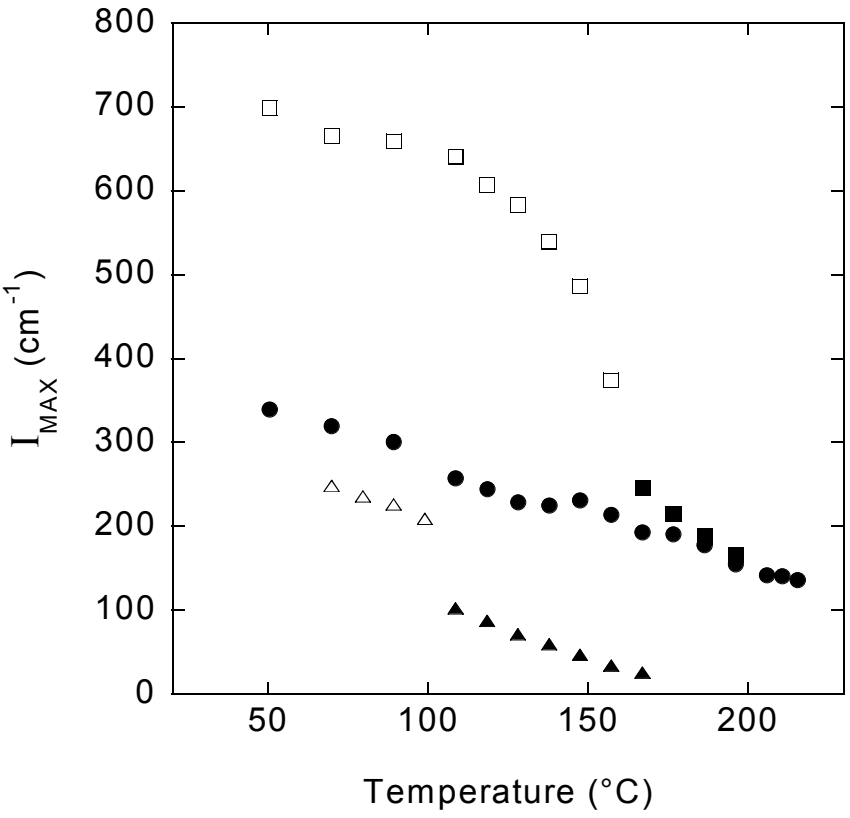
800
700
600
500
400
300
200
100
0
50
100
150
200
I_{MAX} (cm^{-1})
Temperature (°C)

Figure 7

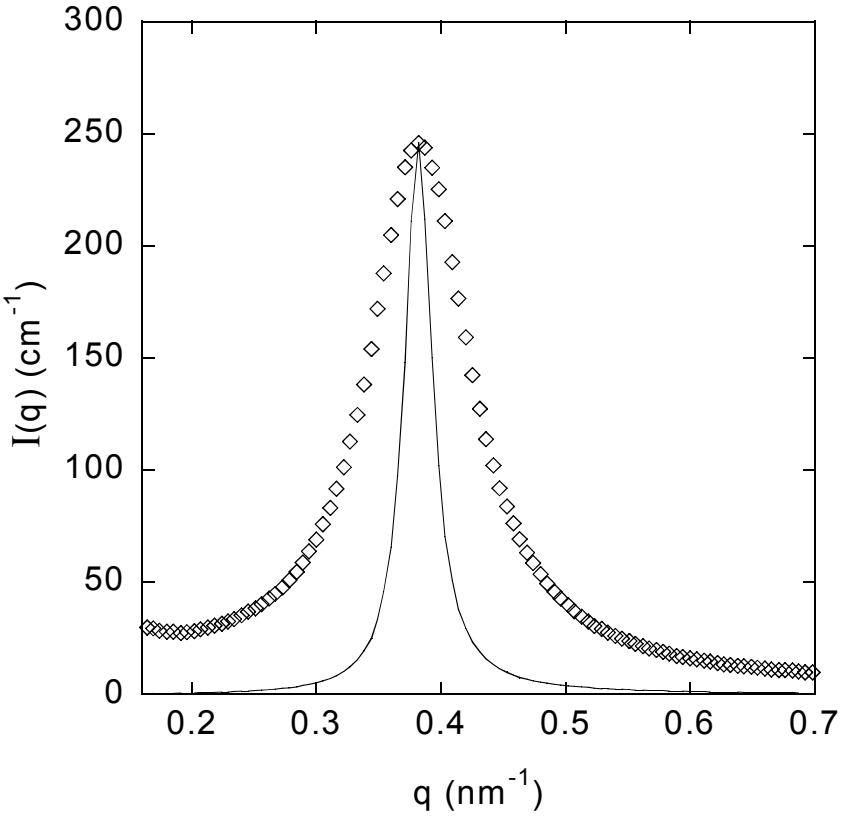

Figure 8

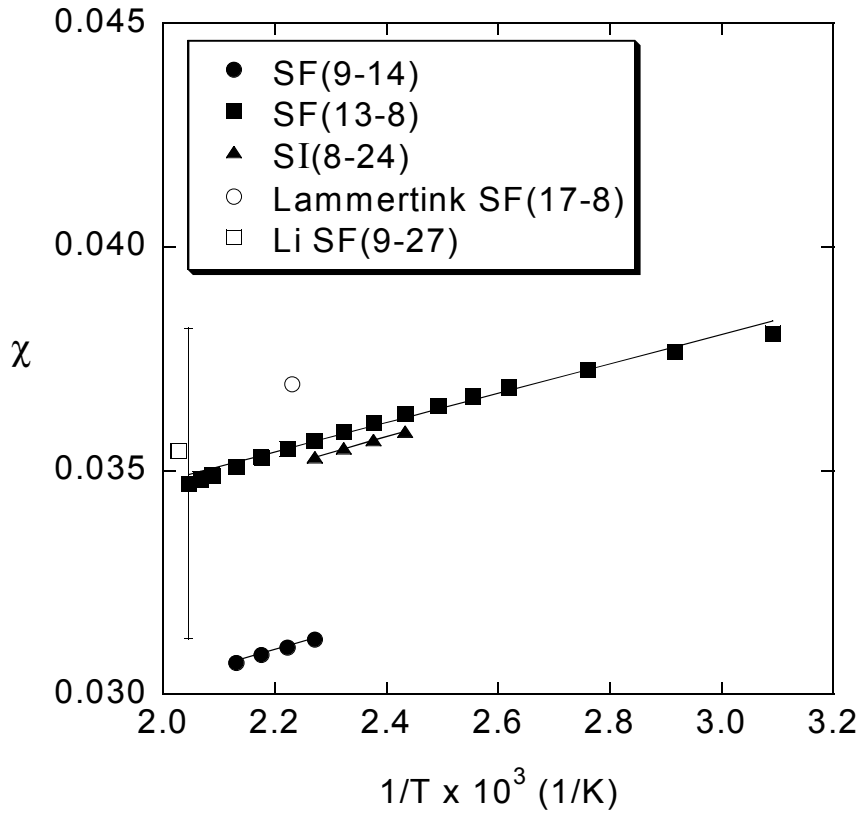
0.045
0.040
0.035
0.030
χ
SF(9-14)
SF(13-8)
SI(8-24)
Lammertink SF(17-8)
Li SF(9-27)
2.0
2.2
2.4
2.6
2.8
3.0
3.2
1/T x 10^3 (1/K)

Figure 9

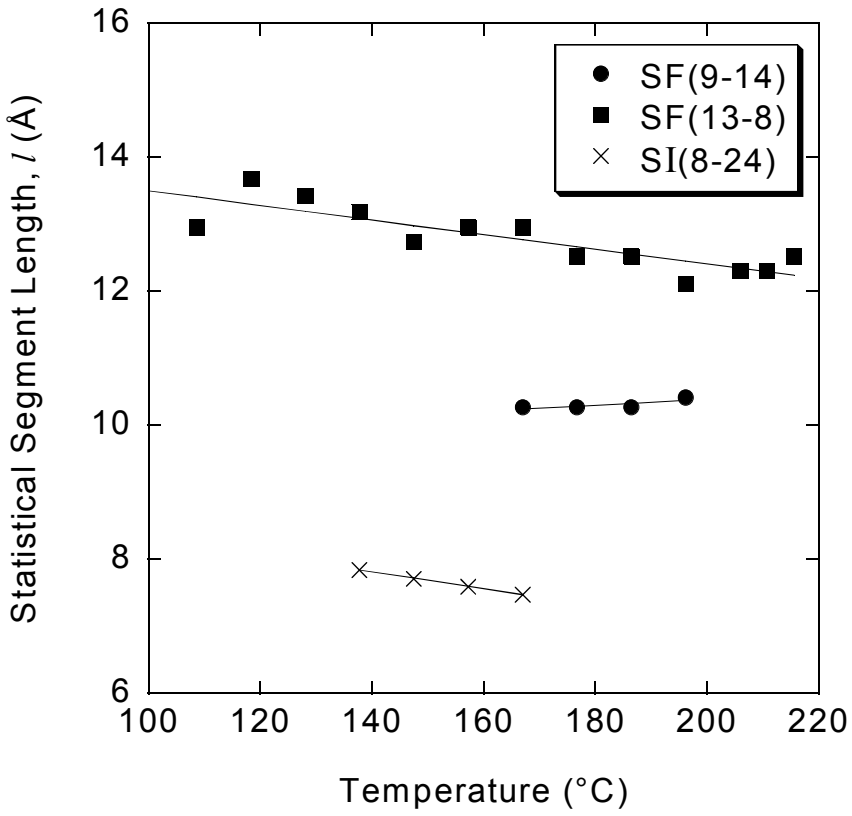
16
14
12
10
8
6
100
120
140
160
180
200
220
Statistical Segment Length, l (Å)
Temperature (°C)
SF(9-14)
SF(13-8)
SI(8-24)

Figure 10

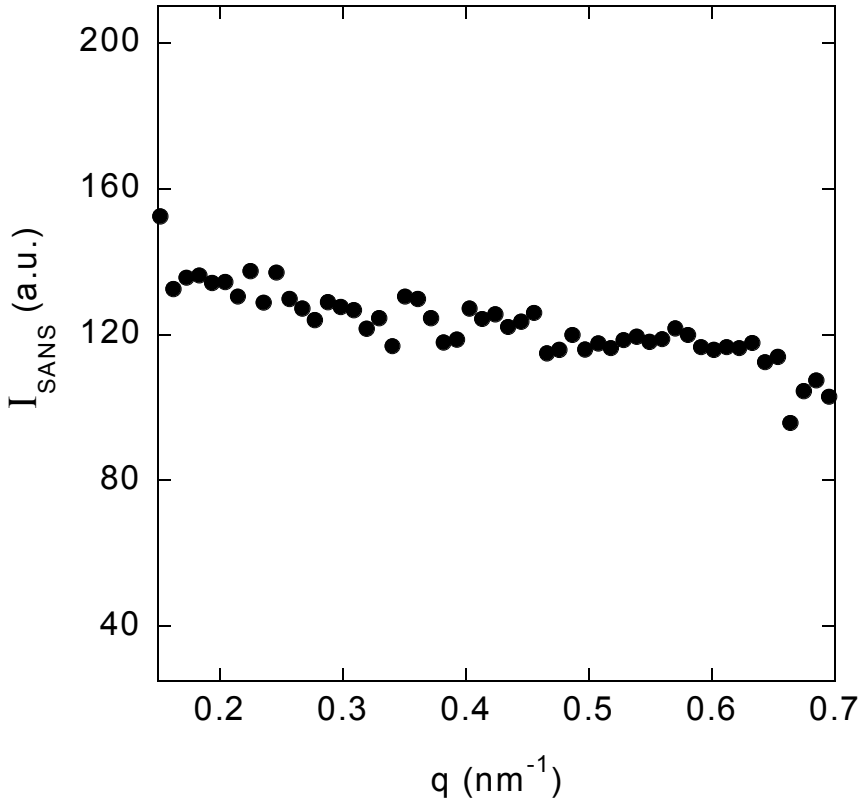
200
160
120
80
40
I_{SANS} (a.u.)
0.2
0.3
0.4
0.5
0.6
0.7
q (nm^{-1})

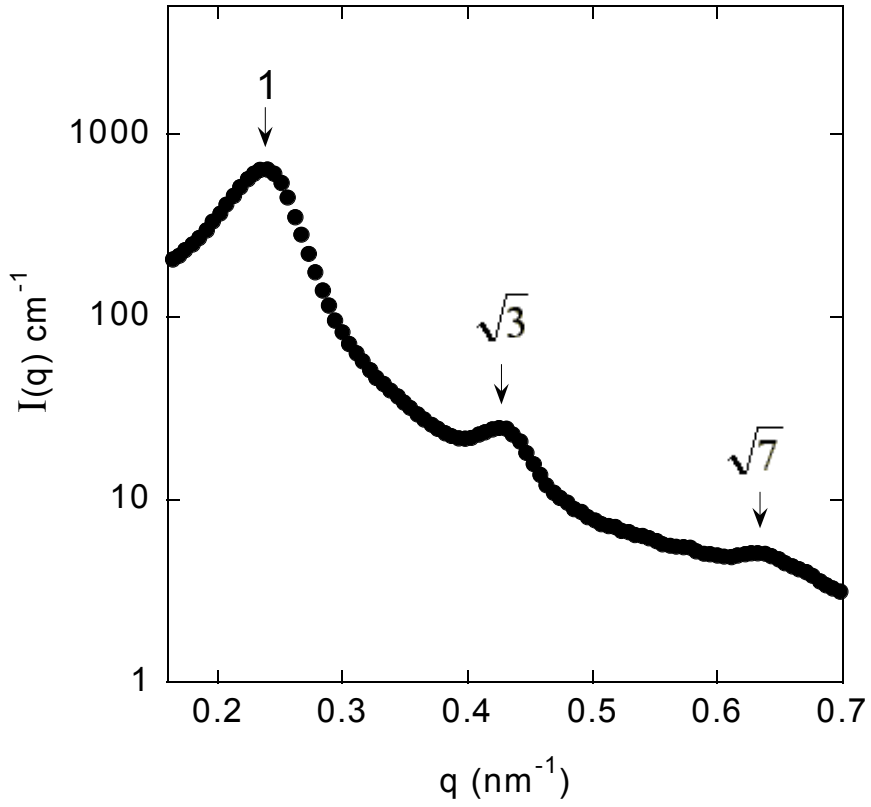
1
1000
100
10
1
I(q) cm^{-1}
$\sqrt{3}$
$\sqrt{7}$
0.2
0.3
0.4
0.5
0.6
0.7
q (nm^{-1})